

pubs.acs.org/JACS Communication

Enantio- and Diastereodivergent Cyclopropanation of Allenes by Directed Evolution of an Iridium-Containing Cytochrome

Brandon J. Bloomer, Isaac A. Joyner, Marc Garcia-Borràs, Derek B. Hu, Martí Garçon, Andrew Quest, Consuelo Ugarte Montero, Isaac F. Yu, Douglas S. Clark, and John F. Hartwig*



Cite This: J. Am. Chem. Soc. 2024, 146, 1819-1824



ACCESS I

III Metrics & More

Article Recommendations

SI Supporting Information

ABSTRACT: Alkylidene cyclopropanes (ACPs) are valuable synthetic intermediates because of their constrained structure and opportunities for further diversification. Although routes to ACPs are known, preparations of ACPs with control of both the configuration of the cyclopropyl (R vs S) group and the geometry of the alkene (E vs E) are unknown. We describe enzymatic cyclopropanation of allenes with ethyl diazoacetate (EDA) catalyzed by an iridium-containing cytochrome (Ir(Me)-CYP119) that controls both stereochemical elements. Two mutants of Ir(Me)-CYP119 identified by 6-codon (6c, VILAFG) saturation mutagenesis catalyze the formation of (E)-ACPs with -93% to >99% ee and >99:1 E/Z ratio with just three rounds of 96 mutants. By four additional rounds of mutagenesis, an enzyme variant was identified that forms (E)-ACPs with up to 94% ee and a 28:72 E/Z ratio. Computational studies show that the orientation of the carbene unit dictated by the mutated positions accounts for the stereoselectivity.

lkylidene cyclopropanes are both natural¹ and synthetic² A constrained ring compounds (Figure 1a) that can react at the alkene unit and that possess unusual stereochemistry and geometric relationships between substituents. The cyclopropanation of a monosubstituted allene with an unsymmetrical carbene can produce eight isomeric products (Figure 1b), and several features of allenes make the cyclopropanation of them a challenging transformation to achieve stereoselectively. First, allenes are less reactive than alkenes toward cyclopropanation, due to the diminished nucleophilicity resulting from the electron-deficient central sp carbon. Second, reaction with the terminal olefin of terminal allenes is favored sterically, but reaction at the internal olefin is favored electronically. Finally, the two faces of the terminal alkene of a 1,1-disubstituted, unsymmetrical allene are diastereotopic and lead to (E)- and (Z)-configurations of the products. Thus, only five examples of undirected, enantioselective cyclopropanation of achiral allenes with ee >90% have been reported, 3-7 despite a rich history of stereochemical studies of ACPs, and these five examples circumvent the aforementioned challenges by using a carbene that is sterically bulky^{3,4} or that contains a second binding site for the metal and an excess of allene.⁵ Because few allenes are commercially available, selective cyclopropanation with a limiting allene is the appropriate stoichiometry for synthetic applications. Intermolecular, enantioselective cyclopropanation of allenes to form the (Z)isomer as the major product is unknown.

We envisioned that a carbene transferase, which can be modified by directed evolution, could catalyze this reaction to form the various isomers stereoselectively. Our group has published several challenging carbene transfer reactions catalyzed by iridium-containing cytochromes, including one based on CYP119 (herein abbreviated as Ir(Me)-CYP119). These artificial metallo enzymes (ArMs) catalyze cyclo-

propanations of unconjugated alkenes, including sterically hindered aliphatic alkenes that resist reactions catalyzed by small-molecule or natural enzymatic systems or react with low ee. 8,9 Thus, we considered that such enzymes could catalyze the cyclopropanation of allenes. Here, we report that an Ir(Me)-CYP119 variant identified by directed evolution in whole cells catalyzes regioselective cyclopropanation of allenes with EDA to form (E)- or (Z)-isomers with high enantioselectivity.

Our studies with an Ir(Me)-CYP119 catalyst for allene cyclopropanation began with the protein CYP119.gen0, which contains C317G, L155W, T213G, and V254L mutations of wild type CYP119, and the combination of phenylallene and EDA as the model substrates. This mutant previously catalyzed the stereoselective cyclopropanation of carvone.^{8,10} The reaction with phenylallene produced a mixture of alkylidene cyclopropane isomers (1a/1b/1c = 78:10:12). The geometry of the major isomer in the crude reaction was assigned unambiguously by 2D correlation and NOESY NMR spectroscopy and comparison to published spectra¹¹ as (E) (see Supporting Information, Figure S1). Signals assigned to the (Z)-isomer in the mixture also matched those reported previously.¹¹ Encouraged by these results, we conducted the directed evolution of CYP119 to increase the selectivity for the (E)- and (Z)-ACP products.

Received: November 20, 2023
Revised: December 29, 2023
Accepted: December 29, 2023
Published: January 8, 2024





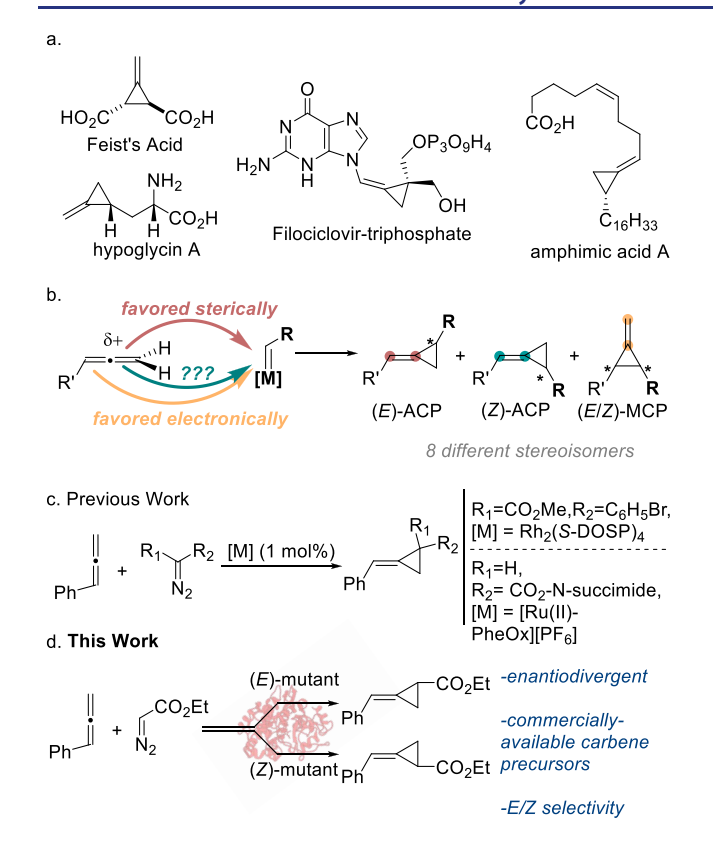


Figure 1. (a) Representative natural and synthetic ACPs, (b) challenges of allene cyclopropanation, (c) previous enantioselective cyclopropanation of allenes, and (d) enzymatic, *E/Z*-tunable, enantioselective cyclopropanation of allenes with EDA. ACP = alkylidene cyclopropane, MCP = methylene cyclopropane.

To identify variants of CYP119 that are more selective for each olefin geometry, we screened mutant libraries using E. coli engineered to assemble Ir(Me)-CYP119 in vivo¹² and enable directed evolution without the purification of individual artificial metalloenzymes (ArMs). We used iterative saturation mutagenesis (ISM) to determine the residues near the active site that would influence reactivity and selectivity using CYP119.gen0 as the parent enzyme. To streamline the discovery of mutants to form each type of product, we limited the scope of typical ISM from all 20 amino acids to six sterically diverse ones (V, I, L, A, F, G) using the mixed mutagenic codons GBT and HTT. Reetz used this six-codon (6c) strategy to vary the lipophilic active site of limonene epoxide hydrolase. 13 By this method, we screened saturation libraries of four sites in one 96-well plate (23 colonies per residue = 98% library coverage). 14

To begin, we selected eight positions in the active site for 6c-mutagenesis (V151, A152, L205, I208, A209, G213, P253, and L354; Figure 2a). The first two residues were located on the F–G loop, the next four on the I-helix just north of the iridium cofactor (Ir(Me)-MPIX), and the last two on parallel loops east of Ir(Me)-MPIX. The first round of evolution showed that the E-(-)-ACP isomer was produced by the A209I mutant (CYP_{E-minus}, Figure 2b) with 93% ee as a single diastereomer. In addition, two single mutations (A152G and G213L) reversed the enantioselectivity to produce (E)-(+)-ACP as a single olefin isomer, and the combination of these two mutations created a second-generation mutant that formed the (E)-(+)-ACP in 94% ee. One subsequent round of mutagenesis gave a mutant (CYP_{E-plus} with an additional I205G

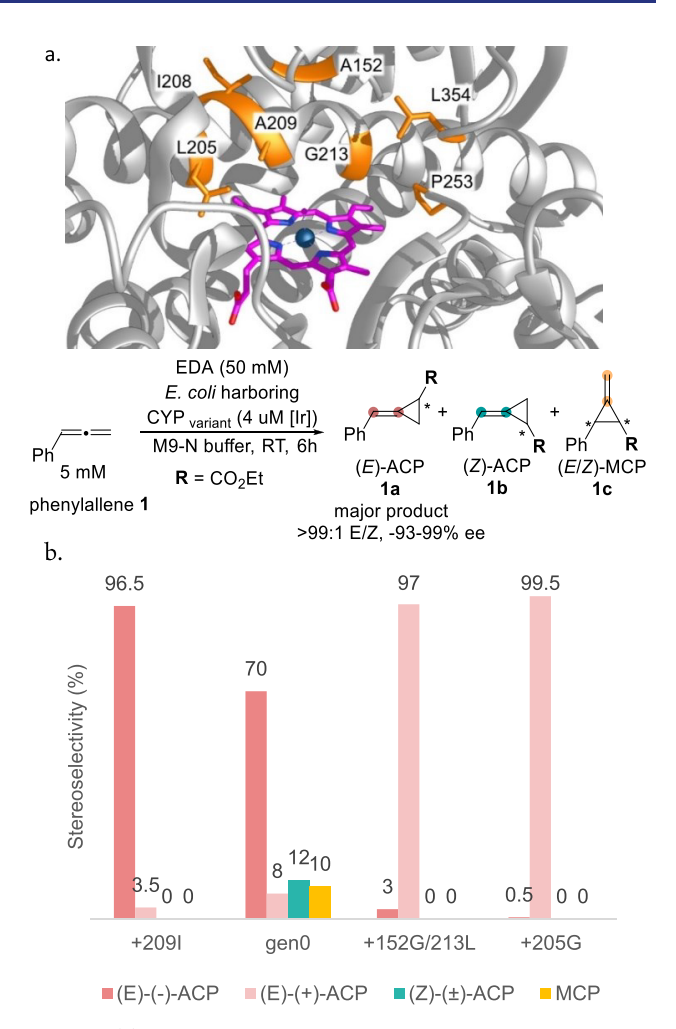


Figure 2. (a) Residues selected for 6-codon saturation mutagenesis. (b) Evolution of CYP119 toward (*E*)-ACP 1a.

mutation) that produced the (E)-(+)-ACP with >99% ee. Thus, the generation and testing of just 384 mutants led to the discovery of $\text{CYP}_{\text{E-minus}}$ and $\text{CYP}_{\text{E-plus}}$.

The (E)-(+)-ACP was prepared on a 1 mmol scale in 69% yield (909 TON) with 97% ee and a 97:1:2 ratio of 1a/1b/1c using the purified CYP_{E-plus} enzyme. This activity and selectivity exceeds that of the reaction catalyzed by Ru^{II}(Pheox), which was conducted with five equivalents of phenylallene and *O*-succinimidyl diazoacetate as the diazo reagent (1 mmol scale, 62% yield, 62 TON, 97% ee, 94:1:5 E/Z/MCP). The (E)-(+)-ACP isomer was determined to be the (R)-enantiomer by X-ray crystallography (see Supporting Information).

We also sought a mutant that would form the (Z)-isomer by targeting four additional positions in the active site (V69, W155, L254, and V353; Figure 3) where the aromatic moiety of the allene was likely to lie. Indeed, the L254V mutation formed an enzyme that produced the (Z)-ACP with a slight enrichment of the (Z)-isomer from 89:11 to 73:27 E/Z and with 40% ee. Three subsequent rounds of 6c-mutagenesis (L205F/G213A/F153V) yielded the mutant CYP_{Z-minus} that produced (Z)-(-)-ACP with the (Z)-isomer as the major one (28:72 E/Z) and with a high 94% ee.

Having identified mutants that are selective for (E)-(+), (E)-(-), and (Z)-(-) stereoisomers, we investigated the effect of allene substituents on the stereoselectivity (Figure 4). CYP_{E-plus}

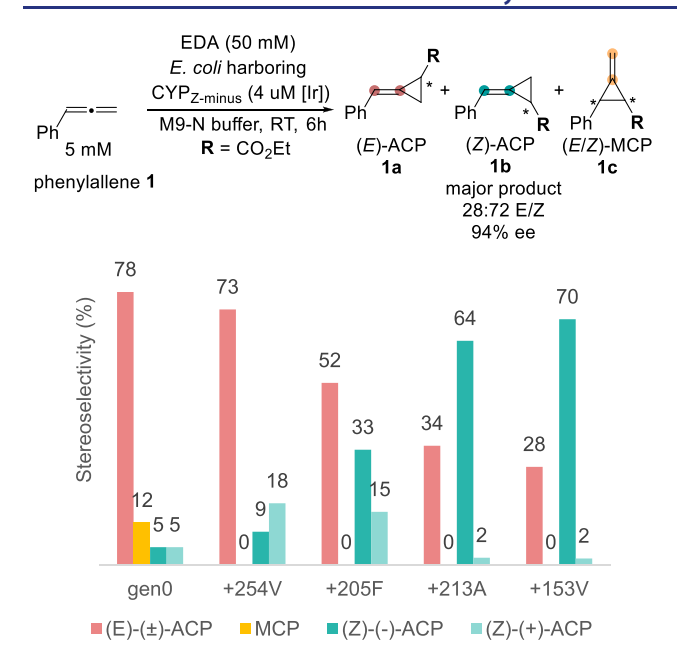


Figure 3. Evolution of CYP119 toward (Z)-ACP 1b.

was tolerant of small fluoro-, methyl-, methoxy-, and chloro-substituents on the aryl group in aryl-ACPs (97–99% ee) and larger *n*-propyl-, bromo-, and *t*-butyl substituents on the aryl group led to only a small decrease in ee (96% ee, 92% ee, and 87% ee, respectively). Aliphatic ACPs with more flexible *n*-hexyl and phenethyl formed the cyclopropane with good ee but with a larger proportion of the methylene cyclopropane (MCP) than from the arylallenes.

To assess the factors controlling stereoselectivity, we conducted DFT calculations and MD simulations. First, DFT calculations were performed on the reaction of allene 1 catalyzed by a free, unsubstituted Ir(Me)-porphine complex to reveal the intrinsic selectivity of the cofactor for the cyclopropanation of phenylallene. The transition-state energies calculated by DFT for cyclopropanation of both terminal and internal double bonds to form E or Z isomers were all within about 1 kcal·mol⁻¹ (see Figure S8). The lowest-energy transition state (ΔG^{\ddagger} of 4.6 kcal·mol⁻¹) led to the (*E*)-ACP product, which was the major observed olefin isomer, but the small differences in calculated ΔG^{\ddagger} demonstrate that the evolved enzyme selectivity is controlled primarily by interactions with amino acid side chains of the active site. Furthermore, the low calculated ΔG^{\ddagger} values (4.6 to 5.7 kcal· mol⁻¹) for these truncated models reflect the high reactivity of the Ir-carbene intermediate toward the allene. These activation barriers are comparable, although slightly higher, than the ΔG^{\ddagger} values (2.2 to 4.7 kcal·mol⁻¹) calculated previously for the cyclopropanation of internal alkenes by the same Ir(Me)(por)carbene unit.10

To understand the regio- and stereoselectivity induced by the evolved enzymes, we conducted molecular dynamics (MD) (see Figures S9 and S10). As previously done, 10 we first evaluated the accessible conformations of the Ir-carbene intermediates in the active sites of the evolved variants, $\rm CYP_{E-minus}$ and $\rm CYP_{E-minus}$ (see Figure S9). MD simulations of the $\rm CYP_{E-minus}$ and $\rm CYP_{E-minus}$ variants with the carbene covalently bound to the Ir(Me)-porphyrin revealed a substantial difference in the orientation of the carbene moiety within the active site of the three enzymes. In the $\rm CYP_{E-minus}$

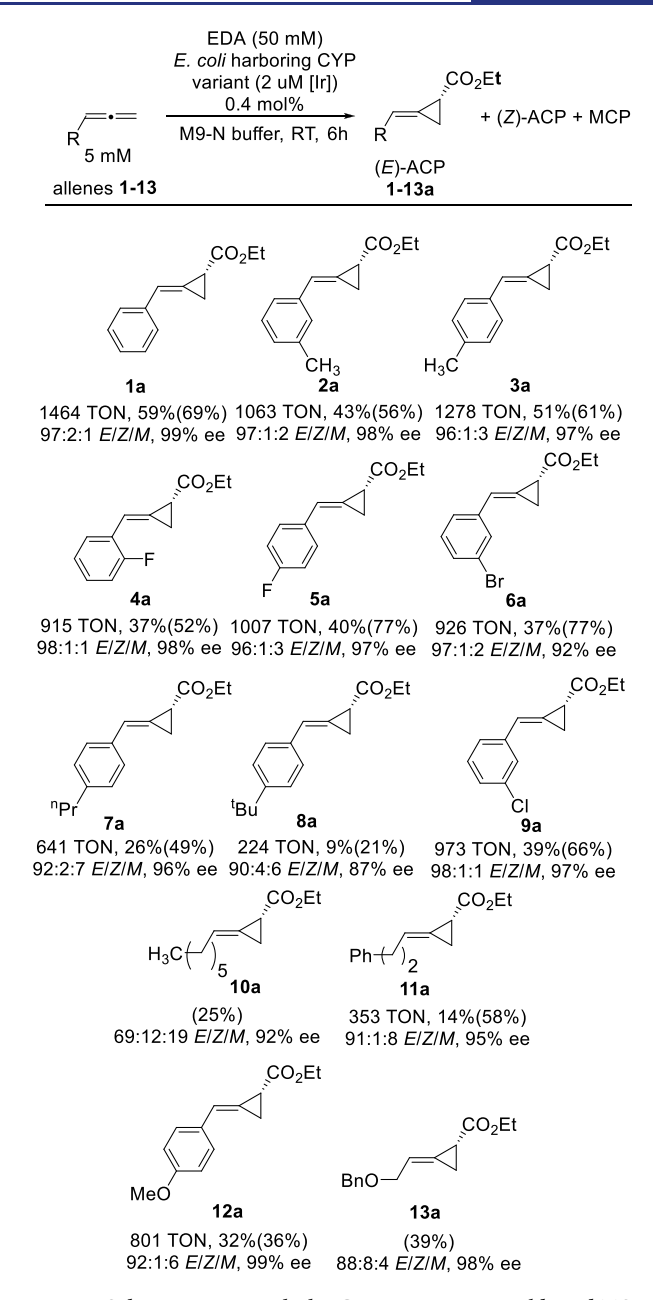
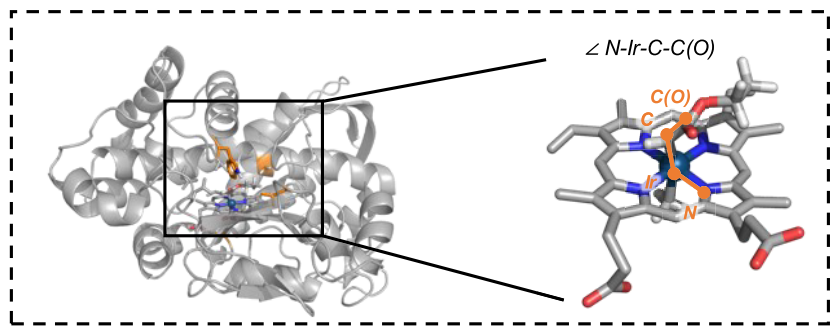


Figure 4. Substrate scope with the CYP_{E-plus} variant. Yields and TON were determined by GC. Isolated yields in parentheses were obtained with the following conditions: 0.075 mol % CYP_{E-plus} 0.5 mmol allene (5 mM), 10 mmol EDA (slow addition over 20h), 100 mM NaCl, 100 mM NaPi, pH 6.0, 0.5% w/v TPGS-750-M.

variant, the ethoxycarbonyl group of the carbene resided near G213 in the MD trajectories, with the opposite side of the active site occupied by the bulkier L69, L205, and I205 side chains (see Figure 5). A similar positioning of Ir-carbene in the active site was observed for the CYP_{z-minus} variant. In contrast, MD simulations indicated that the carbene rotates approximately 100° around the Ir–C bond (see Figures 5 and S9) in the CYP_{E-plus} variant due to the replacement of Gly by Leu at position 213. This mutation positions the ethoxycarbonyl toward the L69 side chain, which is located deeper in the active site cavity because of the space created by the I205G mutation. This difference in orientation of the carbene within the CYP_{E-plus} and CYP_{E-minus} mutants inverts the configuration of the carbene carbon in the product because the pro-(S) face of



Characterization of accessible conformations for Ir-carbene intermediate when formed in the enzyme active site using MD simulations

Ir-carbene bound MD simulations: b. Substrate docking + restrained-MD simulations CYP_{E-plus} $\angle N$ -Ir-C-C(O) = -37.2° 1208 F153 W155 W155 A152G A209 V353 V353 G213L L69 pro-(E)-(+) allene reactive binding mode L254 Representative snapshot Preferential near from replica 1, t = 600 nsSnapshot from replica 1, t = 240 ns attack conformations characterized from CYP_{E-minus} \angle N-Ir-C-C(O) = 72.5° MD simulations F153 1208 A2091 V353 W155 G213 G213 P253 1 69 1 254 pro-(E)-(-) allene

Figure 5. Characterization of (a) Ir-carbene intermediate conformations and (b) reactive allene binding modes, in CYP_{E-plus} and CYP_{E-minus} variants by MD simulations. See Figures S9 and S10 for complete details.

Snapshot from replica 1, t = 300 ns

the carbene reacts with the allene in the $\mbox{CYP}_{\mbox{\scriptsize E-minus}}$ mutant and the pro- (R) face reacts with the allene in the CYP_{E-plus} variant (see Figures 5 and S9).

Representative snapshot

from replica 1, t = 690 ns

To explore how the allene binds and interacts with Ircarbene, we docked allene 1 in the $\text{CYP}_{\text{E-plus}}$ and $\text{CYP}_{\text{E-minus}}$ active sites containing the Ir-carbene. To characterize catalytically relevant binding poses of the substrate, subsequent MD simulations included a geometric restraint that maintained the proximity between the allene and the carbene throughout the MD trajectories, thereby preventing undesired unbinding events and sampling reactive orientations of the carbene and allene (refer to SI and Figure S10 for details). MD simulations with the allene bound suggested that the terminal alkene approaches the carbene in the $\text{CYP}_{\text{E-minus}}$ active site in a near attack conformation that resembled the DFT-optimized (E)-(-)-ACP-TS (Figures 5 and 10). This binding mode of the allene is favored by hydrophobic interactions with W155, V151, A152, and V353 residues and steric interactions with its aromatic ring that would be present in a pro-(Z) binding mode.

In summary, we have shown that an artificial metalloenzyme containing Ir in the active site of a P450 catalyzes the cyclopropanation of allenes and that such ArMs assembled in whole cells can be evolved with libraries generated by 6cmutagenesis to form (E)-(R)-ACP and (E)-(S)-ACP stereoisomers with good selectivity and even to form one major enantiomer of the (Z) isomer that has not been formed with small-molecule catalysts previously. Density functional theory

reactive binding mode

(DFT) calculations (Figure S8) and molecular dynamics (MD) simulations elucidated how mutations in the active site create steric interactions that control the orientation of the Ircarbene intermediate and create transition states with different energies to form the two enantiomers and transition states to form the two olefin geometries that are distinct from each other, even though the energies to form these two isomers are similar in the absence of the protein. Ultimately, these ArMs provide a new stereoselective route to ACP building blocks for further transformations.

ASSOCIATED CONTENT

Supporting Information

The Supporting Information is available free of charge at https://pubs.acs.org/doi/10.1021/jacs.3c13011.

Experimental procedures, characterization data, and NMR spectra (PDF)

Accession Codes

CCDC 2309994 contains the supplementary crystallographic data for this paper. These data can be obtained free of charge via www.ccdc.cam.ac.uk/data_request/cif, or by emailing data_request@ccdc.cam.ac.uk, or by contacting The Cambridge Crystallographic Data Centre, 12 Union Road, Cambridge CB2 1EZ, UK; fax: +44 1223 336033.

AUTHOR INFORMATION

Corresponding Author

John F. Hartwig — Department of Chemistry, University of California, Berkeley, California 94720, United States; Division of Chemical Sciences, Lawrence Berkeley National Laboratory, Berkeley, California 94720, United States; orcid.org/0000-0002-4157-468X; Email: jhartwig@berkeley.edu

Authors

Brandon J. Bloomer — Department of Chemistry, University of California, Berkeley, California 94720, United States; Division of Chemical Sciences, Lawrence Berkeley National Laboratory, Berkeley, California 94720, United States; Present Address: Merck Center for Catalysis, Princeton University, Princeton, New Jersey, 08544, United States

Isaac A. Joyner – Department of Chemistry, University of California, Berkeley, California 94720, United States; Division of Chemical Sciences, Lawrence Berkeley National Laboratory, Berkeley, California 94720, United States

Marc Garcia-Borràs – Institut de Química Computacional i Catàlisi (IQCC) and Departament de Química, Universitat de Girona, Girona 17003, Spain; orcid.org/0000-0001-9458-1114

Derek B. Hu — Department of Chemistry, University of California, Berkeley, California 94720, United States Martí Garçon — Department of Chemistry, University of California, Berkeley, California 94720, United States; Division of Chemical Sciences, Lawrence Berkeley National Laboratory, Berkeley, California 94720, United States;

orcid.org/0000-0002-3214-0150

Andrew Quest – Department of Chemistry, University of California, Berkeley, California 94720, United States

Consuelo Ugarte Montero – Department of Chemistry, University of California, Berkeley, California 94720, United States Isaac F. Yu — Department of Chemistry, University of California, Berkeley, California 94720, United States; orcid.org/0000-0001-9659-2204

Douglas S. Clark — Molecular Biophysics and Integrated Bioimaging, Lawrence Berkeley National Laboratory, Berkeley, California 94720, United States; Department of Chemical and Biomolecular Engineering, University of California, Berkeley, California 94720, United States; orcid.org/0000-0003-1516-035X

Complete contact information is available at: https://pubs.acs.org/10.1021/jacs.3c13011

Funding

This work was supported by the NSF (CBET-2027943) and the Spanish MICINN (Ministerio de Ciencia e Innovación) PID2019-111300GA-I00, PID2022-141676NB-I00 and TED2021-130173B-C42 projects, and RYC 2020-028628-I grant (to M.G.B), and the Generalitat de Catalunya AGAUR 2021SGR00623 project (to M.G.B.). M.G. thanks EMBO for a postdoctoral fellowship (EMBO ALTF 1001-2021).

Note

The authors declare no competing financial interest.

ABBREVIATIONS

EDA, ethyl diazoacetate; CYP, cytochrome P450; DFT, density functional theory; MD, molecular dynamics; TON, turnover number; ACP, alkylidene cyclopropane; MCP, methylidene cyclopropane; TS, transition state; ee, enantiomeric excess; ISM, iterative saturation mutagenesis

REFERENCES

- (1) Gray, D. O.; Fowden, L. alpha-(Methylenecyclopropyl)glycine from Litchi seeds. *Biochem. J.* **1962**, 82 (3), 385–9.
- (2) Brandi, A.; Goti, A. Synthesis of Methylene- and Alkylidenecy-clopropane Derivatives. *Chem. Rev.* **1998**, *98* (2), 589–636.
- (3) Gregg, T. M.; Farrugia, M. K.; Frost, J. R. Rhodium-Mediated Enantioselective Cyclopropanation of Allenes. *Org. Lett.* **2009**, *11* (19), 4434–4436.
- (4) Gregg, T. M.; Algera, R. F.; Frost, J. R.; Hassan, F.; Stewart, R. J. Substituent effects on rates of rhodium-catalyzed allene cyclopropanation. *Tetrahedron Lett.* **2010**, *51* (49), 6429–6432.
- (5) Chanthamath, S.; Chua, H. W.; Kimura, S.; Shibatomi, K.; Iwasa, S. Highly Regio- and Stereoselective Synthesis of Alkylidenecyclopropanes via Ru(II)-Pheox Catalyzed Asymmetric Inter- and Intramolecular Cyclopropanation of Allenes. *Org. Lett.* **2014**, *16* (12), 3408–3411.
- (6) Hasegawa, Y.; Cantin, T.; Decaens, J.; Couve-Bonnaire, S.; Charette, A. B.; Poisson, T.; Jubault, P. Catalytic Asymmetric Syntheses of Alkylidenecyclopropanes from Allenoates with Donor-Acceptor and Diacceptor Diazo Reagents. *Chem. Eur. J.* **2022**, 28 (47), e202201438.
- (7) Lindsay, V. N. G.; Fiset, D.; Gritsch, P. J.; Azzi, S.; Charette, A. B. Stereoselective Rh₂(S-IBAZ)₄-Catalyzed Cyclopropanation of Alkenes, Alkynes, and Allenes: Asymmetric Synthesis of Diacceptor Cyclopropylphosphonates and Alkylidenecyclopropanes. *J. Am. Chem. Soc.* **2013**, *135* (4), 1463–1470.
- (8) Key, H. M.; Dydio, P.; Liu, Z.; Rha, J. Y. E.; Nazarenko, A.; Seyedkazemi, V.; Clark, D. S.; Hartwig, J. F. Beyond Iron: Iridium-Containing P450 Enzymes for Selective Cyclopropanations of Structurally Diverse Alkenes. ACS Central Science 2017, 3 (4), 302–308
- (9) Natoli, S. N.; Hartwig, J. F. Noble-Metal Substitution in Hemoproteins: An Emerging Strategy for Abiological Catalysis. *Acc. Chem. Res.* **2019**, *52* (2), 326–335.

- (10) Bloomer, B. J.; Natoli, S. N.; Garcia-Borràs, M.; Pereira, J. H.; Hu, D. B.; Adams, P. D.; Houk, K. N.; Clark, D. S.; Hartwig, J. F. Mechanistic and structural characterization of an iridium-containing cytochrome reveals kinetically relevant cofactor dynamics. *Nature Catalysis* **2023**, *6* (1), 39–51.
- (11) Sang, R.; Yang, H.-B.; Shi, M. DBU-mediated transformation of arylmethylenecyclopropenes to alkylidenecyclopropanes. *Tetrahedron Lett.* **2013**, *54* (28), 3591–3594.
- (12) Gu, Y.; Bloomer, B. J.; Liu, Z.; Chen, R.; Clark, D. S.; Hartwig, J. F. Directed Evolution of Artificial Metalloenzymes in Whole Cells. *Angew. Chem., Int. Ed.* **2022**, *61* (5), e202110519.
- (13) Sun, Z.; Salas, P. T.; Siirola, E.; Lonsdale, R.; Reetz, M. T. Exploring productive sequence space in directed evolution using binary patterning versus conventional mutagenesis strategies. *Bioresources and Bioprocessing* **2016**, 3 (1), 44.
- (14) Kille, S.; Acevedo-Rocha, C. G.; Parra, L. P.; Zhang, Z.-G.; Opperman, D. J.; Reetz, M. T.; Acevedo, J. P. Reducing Codon Redundancy and Screening Effort of Combinatorial Protein Libraries Created by Saturation Mutagenesis. *ACS Synth. Biol.* **2013**, 2 (2), 83–92.